Mechanics of Advanced Composite Structures 10 (2023) 247 – 256

Semnan University

Mechanics of Advanced Composite Structures

journal homepage: http://MACS.journals.semnan.ac.ir

Design and Experimental/Numerical Analysis of Metal-Composite Vessel with Spherical Cap under Internal Pressure

J. Mirzaei *, M. Nouri Niyaraki, H.R. Zarei

Department of Aerospace Engineering, Shahid Sattari Aeronautical University of Science and Technology, Tehran, 1384673113, Iran

KEYWORDS

Composite vessel;
Internal pressure;
Spherical cap;
Numerical analysis;
Experimental analysis.

ABSTRACT

Composite vessels are widely used in industry due to their high strength and low weight. In this research, a composite vessel with a metal liner was designed, manufactured, and subjected to internal pressure. The liner of the tank is made of 304 steel, which is screwed on its main part with two patterns of polar and peripheral twisting. In this research, S-glass fibers and epoxy resin 5052 were used. The vessel was subjected to a pressure of 40 bars. Electric strain gauges were used to measure the strain, and stresses were calculated using Hooke's law. In addition to the experimental method, the vessel was also analyzed numerically. ABAQUS (finite element) software was used to examine the experimental data, and the simulation results showed good consistency with the experimental data. The results of the numerical analysis determined the location of the strain gauges. The results of the two methods were compared and discussed. It was found that at low pressures (pressures lesser than 40 bar), composites do not have a significant role in tolerating vessel stress. It has been observed that changes in the geometry of the structure (the joint of the spherical part and the cylinder) resulted in turbulences in the strain and stress curves near the change site.

1. Introduction

A CNG vessel is mainly a seamless cylinder with spherical caps at both ends of the cylinder. According to ISO 11439, CNG vessels fall into four categories. The first type is metal vessels. These types of vessels are seamless and made of steel or aluminum. These vessels are manufactured using spinning or deep drawing methods and have more weight than other vessels. Their mass-to-volume ratio is between 1.2 to 1.54 kg per liter [1]. In the second type, the metal liner is constrained by composite winding layers. This type of vessel has a metal liner made of seamless steel or aluminum, and the cylindrical part of this liner is wrapped by fibers of glass, armid, carbon, or a mixture of them impregnated with resin [2, 3]. The third type of vessel is a fully wrapped metallic pressure vessel. These vessels have a metal liner, and fiberglass composite fibers are fully wrapped around the liner. The ratio of mass to volume is between 0.7 to 1.4 kg per liter [4, 5]. This vessel possesses a liner made of seamless steel or aluminum, and all of this liner is wrapped using helical and hoop winding patterns with fibers of glass, armid, carbon, or a mixture of them impregnated with resin [6, 7]. The composite structure enables decreasing the thickness of the metal part of the liner, and thus, this vessel is lighter than type 1 and 2 vessels. Their ratio of mass to volume is 0.5- 0.7 kg per liter [8]. Type 4 vessels have a plastic liner. These types of vessels have a seamless polymer liner and all internal liners are wrapped by fibers of glass, armid, carbon, or a mixture of them impregnated with resin [1, 4]. The liner is usually made of compressed polyethylene plastic. These types of vessels are wrapped using helical and hoop winding patterns with composite fibers and can be manufactured in larger dimensions and diameters. For this type of vessel, the mass-to-volume ratio is 0.35-0.50 kg per liter [1, 9].

Many researchers have studied the behavior of different types of vessels under different conditions. Hong et al. studied filament-wound composite structures by changing the winding angles through the thickness direction [10-14].

* Corresponding author. Tel.: +98-912-8938440
E-mail address: mirzaei.jaber@yahoo.com

DOI: 10.22075/macs.2022.28318.1432
Received 2022-09-06; Received in revised form 2022-11-28; Accepted 2022-12-24

The optimization of a Type 3 pressure vessel with the aim of decreasing its weight was done by Kim et. al. [15] by obtaining a relation for winding and naming it quasi-geodesic, using a genetic algorithm. They used a program called PREAFT, which connects to ABAQUS software, entered the data into this software, and then obtained good results by using two types of elements and different failure theories. They also found satisfactory results in another paper using a modified genetic algorithm [16]. Mertini et al. [17] examined the effect of applying tow tension during filament winding on the volume percentage of glass-fiber-reinforced polymeric composite tubular. They also investigated the performance of the pressure vessel under different load ratios.

Pei et al. [18] investigated an analytical model for stress and deformation of fiber-reinforced composite filament winding under multiple combined loads and proposed a new method for calculating stresses on vessels under multiple combined loads. Polini and Sorrentino [19] investigated the effects of winding speed and winding trajectory on fiber tension and concluded that by controlling the winding speed and determining its optimal value, the winding tension could be kept near the nominal value that has been intended. Zhao et al. [20] investigated the effect of applying tension on the chemical activity of resin due to changes in its viscosity. Using a program in the ABAQUS software, they modeled this process for a cylinder and studied the percentage changes in the fibers and the temperature changes caused by the start of cooking.

Choi et al. [21] used ANSYS software to analyze a Type 2 composite vessel produced by the deep drawing method. The vessel was made of steel liner, fiberglass, and epoxy fiber composites. Kabir [22] investigated the third type of composite vessel by considering the load-bearing capacity of the metal liner. In this paper, a geodesic winding pattern using grids was adopted. After calculating the thicknesses and modeling the vessel with different geometries of the dome area of the vessel, the obtained longitudinal and radial stress diagrams were drawn using the NISA software.

Wang et al. [23] investigated a type 3 vessel possessing an aluminum and composite liner with two longitudinal layers 2.6 mm thick and a 2.9-mm circumferential layer with similar properties to Kevlar and epoxy composites under autofrettage pressure. They used the ADINA software and a two-dimensional solid element. Amraee Rad et al. [24] designed and analyzed a metal composite vessel under internal pressure. They used the ABAQUS software for the analysis of the data. It was found that the netting analysis method was not optimal and resulted in increased cost and weight of the vessel. In addition, using a softer liner was found to result in further use of the composite properties which may yield better performance in special applications. It was suggested that the complexity associated with designing metal composite pressure vessels can be significantly reduced by using the finite element simulation method.

Onder et al. [25] studied the optimal angle-ply orientations of symmetric and antisymmetric designed shells and tested them experimentally. They continuously changed the pressure during the test and by changing the temperature and winding angle, obtained different results. To find the optimal angle, they compared the results using the finite element method, and their results were confirmed using the Tsai-Wu criteria and the theory of maximum stress and strain. Zu et al. [26] asserted that the most important issue in designing an optimal composite vessel is the optimal design of its profile. Using the classical plate theory and Tsai-Wu failure criterion, they examined the stress contours created in different profiles. They did not use the geodesic winding trajectory. Different coefficients of friction in different profiles were analyzed, and a significant effect of using a non-geodesic trajectory was confirmed. Koussios et al. [27] investigated the applications of vessels under friction tests. The surface quality of the mandrel and the type of winding process (using wet versus dry fibers) significantly affected the outcomes. The effect of fiber speed, roving tension, and fiber material, however, was not significant. In this research, the investigation and construction of vessels used in different industries have been discussed. In this research, by achieving acceptable numerical results, there is no need to test prototypes in the production process, which reduces production costs. In this research, a composite vessel with a metal liner was designed, manufactured, and subjected to internal pressure. The liner of the tank is made of 304 steel, which is screwed on its main part with two patterns of polar and peripheral twisting. In this research, S-glass fibers and epoxy resin 5052 were used. The vessel was subjected to a pressure of 40 bars. Electric strain gauges were used to measure the strain, and stresses were calculated using Hooke's law. In addition to the experimental method, the vessel was also analyzed numerically.

2. Experimental

2.1. Manufacturing Vessel Liner

In this research, a composite vessel with a metal liner was designed, manufactured, and subjected to internal pressure. The liner of the

tank is made of 304L steel (Table 1), which is screwed on its main part with two patterns of polar and peripheral twisting. In this research, S-glass fibers and epoxy resin 5052 were used (Table 2).

Table 1. Typical compositions for the metal (wt%)

Element	Fe	Ni	Cr	C	S	Si	Mn	P
AISI 304	Rem	8-11	18-20	0.08	0.03	1	2	0.045

Table 2. Mechanical properties of composites

Properties	Composite
E_{11} (GPa)	43
E_{22} (GPa)	8.9
G_{12} (GPa)	4.5
ν_{12}	0.27
X_t (MPa)	1280
X_c (MPa)	690
Y_t (MPa)	49
Y_c(MPa)	158

There are several ways to make a liner, and in this study, the cold spinning method was used to reduce costs and make the manufacturing process more economical. This method, which serves as a cold-forming process of metals (cold work), is one of the oldest methods and has been done manually for many years. Using this method, cooled materials can be manufactured with more precise tolerances and smooth surfaces, but it is a costly process as it requires more force to deform the metal. In industrial sectors, the initial cross-section reduction is done at a very high temperature, and the final reduction is done at a lower temperature to take advantages of both processes. In this method, the metal sheet is drawn on a rotating mandrel to take its shape. To calculate the liner thickness, an experimental relation was applied (Equation 1) [26].

$$t \geq \frac{D}{250} + 1 \tag{1}$$

where D is the vessel diameter and t is the liner thickness. Given that the diameter of the vessel was 158 mm, the minimum thickness of the liner is 1.6 mm. In the design of the vessel, the thickness of the liner was considered to be 1.6 mm. Figure 1 shows the designed liner.

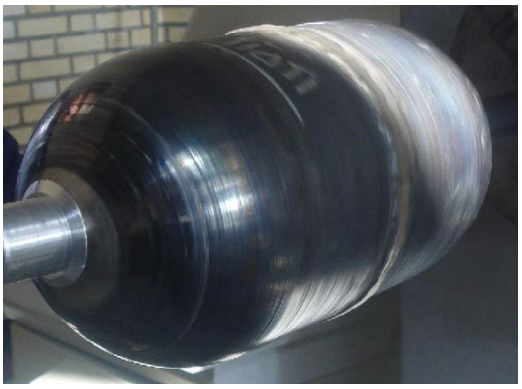

Fig. 1. The designed liner

2.2. Details Determining the Pressure Tolerance of Metal Liner

Since the stresses on the liner are two-dimensional, the Von-Mises stress formula (Equation 2, 3) was applied to determine the pressure tolerance of the liner [26].

$$S_Y{}^2 = \sigma_\theta{}^2 - \sigma_\theta \sigma_X + \sigma_X{}^2 \tag{2}$$

$$S_Y{}^2 = \left(\frac{p.a}{t}\right)^2 - \left(\frac{p.a}{t}\right).\left(\frac{p.a}{2t}\right) + \left(\frac{p.a}{2t}\right)^2 \tag{3}$$

Since the reliability coefficient 3 is considered, to obtain the pressure1, we put one-third of the yield stress (which will be calculated in the next section) in the above relation, and the pressure was obtained P=9.51 MPa. Since the pressure of 210 bars is considered for the vessel, it can be concluded that the pressure borne by the liner is about 45% of the internal pressure of the vessel.

2.3. Determining the Rotation Angle

To determine the rotation angle in this part of the vessel, Equation 4 is used [26]. It is calculated as follows:

$$\alpha = sin^{-1}\frac{2r}{D} = 15.23\ Degrees \tag{4}$$

where r is the radius of the opening of the vessel, and D is the diameter of the cylindrical part of the vessel. Since the radius of the heads changes continuously, to determine the angle of rotation in this section, the head segment is first divided into several segments and the average radius of each segment is determined. Then the rotation angle of each segment is calculated according to Equation 5 [28].

$$\alpha_e = sin^{-1}\frac{2r}{D_e} \tag{5}$$

where α_e is the rotation angle of each segment, r is the radius of the opening of the vessel, and D_e is the diameter of each segment.

Figure 2 demonstrates the radius-location changes, and Figure 3 shows the rotation angle-location changes.

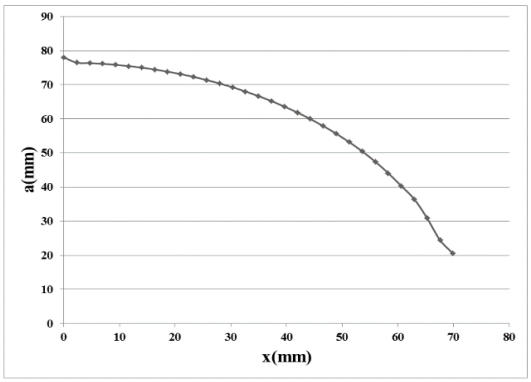

Fig. 2. Changes in the radius of the head segments

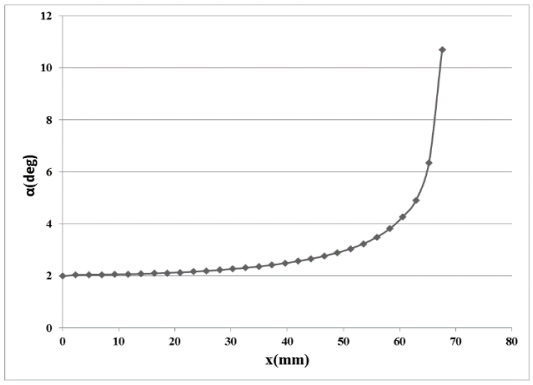

Fig. 3. Changes in rotation angle of fibers

2.4. Calculation of Composite Thickness Using the Geodesic Method

Because the vessel used is of type 3, it has 2 types of winding in the cylindrical part, and two values for the thicknesses must be obtained to determine the thickness of the composite in the cylindrical part:

a) The thickness of hoop winding
b) The thickness of helical winding

An algorithm is used to determine the values for the above thicknesses that are related to each other [26]. In this algorithm, first, two initial thicknesses are considered for each of the winding types, and the stiffness matrices and forces applied to the reservoir are calculated. Using the results of these calculations, the strain and stress values of the vessel are calculated, and then the results are entered into the Tsai-Wu formulae. If this relationship is established, the obtained thicknesses are acceptable thicknesses, otherwise, these steps will continue. It is noteworthy that at the stage when the Tsai-Wu relationship was established, this process can be continued to optimize this thickness. After performing the above steps and optimization, the following values for the thicknesses were obtained 2 mm for hoop and helical winding.

To calculate the thickness of the head, the two following assumptions are made:

a) The volume ratio of fibers remains constant.
b) The number of fibers in the vertical cross-section is constant.

Drawing on these two assumptions, the thickness in the longitudinal direction is obtained using Equation 6 [26]:

$$t = \frac{r_c cos\alpha_c}{r\ cos\alpha} * t_c \quad (6)$$

where r_c the radius of the cylindrical part is, α_c is the rotation angle, and t_c is the thickness of the cylindrical part.

As mentioned in the previous section, the geodesic method has been used for the winding. In this method, because the rotation angle and radius of the vessel are constant, the thickness of the composite in the cylindrical part does not change. However, since both the radius and rotation angle change in the heads, the segmentation of the previous part is used to determine the thicknesses.

3. Numerical Analysis of Metal-Composite Vessel

The analysis of metal-composite vessels' pressure is one of the most challenging issues in mechanical engineering. With the development of numerical and finite element methods and tremendous progress in computer science, the role of analytical methods in solving these types of problems has been gradually reduced. In recent years, researchers around the world have extensively used the finite element method to explain the behavior of these types of vessels. One of the best-known software in this field is ABAQUS software.

3.1. Vessel Modeling

In the current study, for modeling the vessel, first, the rotation angle was defined as a unit in the cylindrical part due to the constant thickness of the metal liner and the composite. Considering that there is a hoop welding in the center of the cylinder, to model the vessel cylinder with ABAQUS software, at each step, half of the cylinder part is modeled, then both halves were placed together. An 8-node S8R element is used for vessel meshing. The reason for using this element is to show well the changes of stress and strain in the thickness of the shell. Also, several factors have been specially considered in determining the number of meshes during meshing. As mentioned earlier, the thickness of the composite and the rotation angle are not fixed in the head segment. Therefore, the segmentation used in the previous section was considered,

determining the thickness of the liner and the composite as well as the type of materials used in each segment [29]. Also, due to the symmetry of the vessel with respect to the XY plane, half of the vessel is modeled in software to simplify and reduce the amount of software computation. In addition, fiber pre-strain was ignored in vessel modeling. After modeling the vessel using the ABAQUS software, all parts of the vessel must be networked for analysis [30]. The 8-node shell element was used for networking the vessel. This element type was used in this study because it properly represents the stress and strain changes in the shell thickness under loading. Also, using the optimal number of networks while networking the vessel is very important to reduce software computations. So, during this process, the number of networks changes several times until the optimal networking pattern was determined and applied.

Considering the symmetry of the vessel, half of it was modeled for analysis, using the software [20]. For the correct analysis of the plane of symmetry under study, some constraints on the nodes should be considered, which is done in Figure 4.

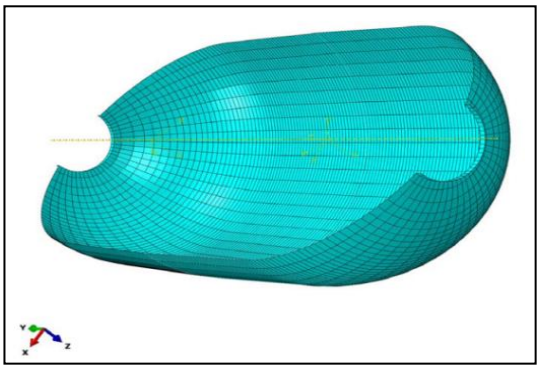

Fig. 4. the vessel with constraints on its surface

Drawing on the finite element analysis, there should be loading on the vessel. Since this study aims to investigate the results of numerical and experimental stress and strain distribution in the elastic region, the loading was performed at a pressure of 40 bars. Figure 5 shows the vessel under loading conditions.

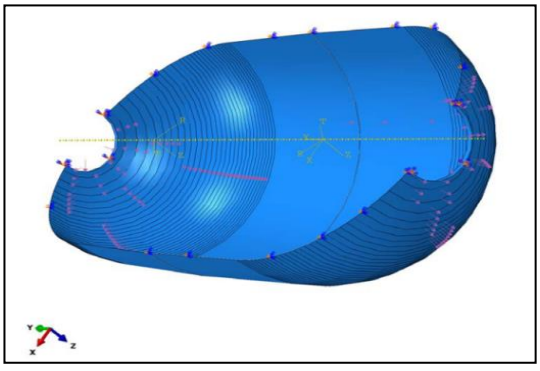

Fig. 5. the vessel under loading conditions

4. Discussion and Analysis of the Results

4.1. Numerical Analysis of Metal-Composite Vessel

Figures 6 and 7 show the numerical values for longitudinal and circumferential strains respectively. Also, the measurement was started from the middle of the cylindrical part of the vessel to its end.

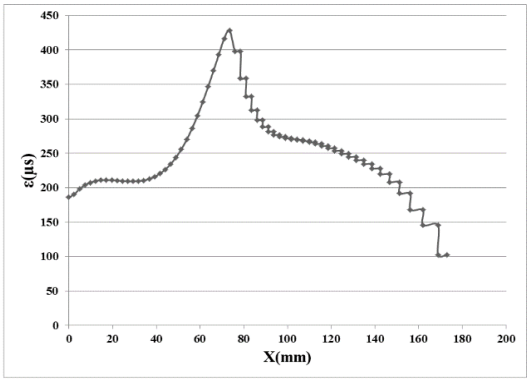

Fig. 6. Numerical analysis of strain distribution of the vessel in the longitudinal direction at a pressure of 40 bars

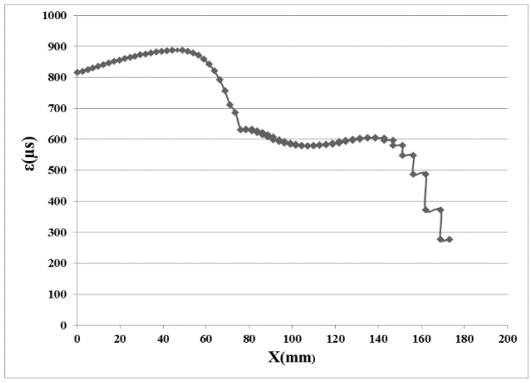

Fig. 7. Numerical analysis of strain distribution of the vessel in the circumferential direction at a pressure of 40 bars

Figures 8 and 9 show numerical values for longitudinal and circumferential numerical stresses, respectively. Also, the measurement was started from the middle of the cylindrical part of the vessel to its end.

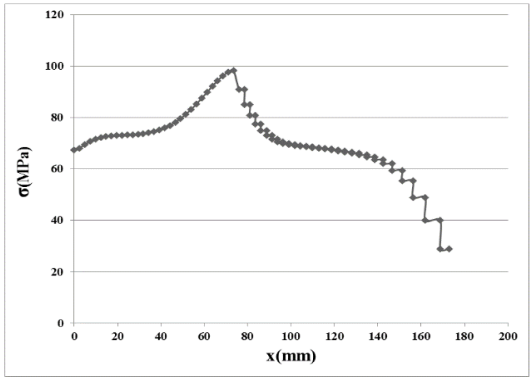

Fig. 8. Numerical analysis of stress distribution of the vessel in the longitudinal direction at a pressure of 40 bars

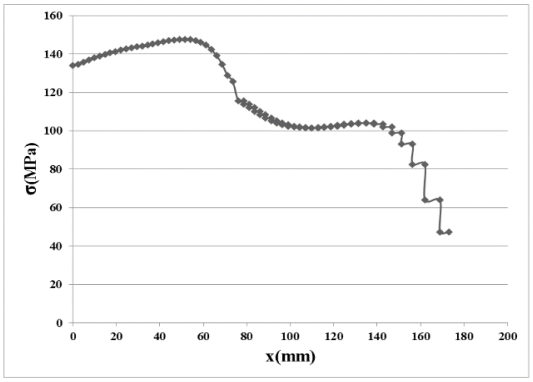

Fig. 9. Numerical analysis of stress distribution of the vessel in the circumferential direction at a pressure of 40 bars

4.2. Experimental Analysis of Metal-Composite Vessel

The results of theoretical methods, whether analytical or numerical, are acceptable if confirmed by experimentation.

Theoretical, analytical, and numerical methods will be the basis of design in practice when they are experimentally verified. Thus, the experimental method (observation and testing) is of significant importance in engineering issues.

The analysis of composite shells is challenging, and it is not possible to solve the differential equations that govern their behavior, so the geometric or numerical solutions always contain different approximations, especially when the structure includes several thin shells. While the vessel under study is a closed structure possessing a simple shape with a cylinder and two hemispherical caps, it does not possess a robust solution.

While there are numerous challenges associated with performing accurate tests on thin-walled composite pressure vessels, this study conducted an experimental analysis of the behavior of the vessels under internal pressure.

The bending method was used to build the vessel. In the process of bending metals, the amount of ultimate strength and yield stress of that metal changes.

To assess the mechanical behavior of the metal after bending, first, two tensile models based on the E8 standard were prepared from the liner and then tested with the INSTRON 5500R tensile device (Figure 10), and using the diagrams, the yield stress and the ultimate strength can be measured.

Figure 11 shows the output diagrams of the first models of the tensile test.

Fig. 10. Tensile testing devices

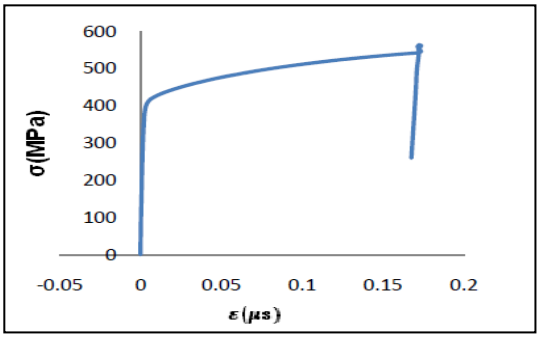

Fig. 11. Tensile test of the first sample

As shown in Figures 12 and 13, using the slope of the curve in the elastic region, the elastic modulus of the metal used in the construction of the vessel can be calculated (E = 155.5 GPa). Also, according to the ASME standard, if we move away from the origin of the stress-strain diagram by 0.2% and draw a line parallel to the line of the elastic region, the intersection of the line with its value diagram will be the yield stress value. Using the maximum values of the above diagrams, the ultimate strength of the metal is calculated, which is equal to $\sigma = 420$ MPa and $\sigma_{UTS} = 520$ MPa.

The area between the yield stress and the failure point of the metal is greatly stretched, which indicates the toughness of the metal. Also, based on the diagram, it can be concluded that the metal under study is close to the elastic-perfectly plastic state. The values for the modulus of elasticity calculated in this test and provided by the company slightly vary. These changes are due to measurement errors, as the modulus of elasticity cannot be changed under these conditions. However, when using mechanical properties in numerical analysis, the modulus of elasticity provided by the manufacturer is used.

A strain gauge is connected to a selector device to measure and read the strain values. The values were displayed by a program on the computer screen. A 16-channel instrument was connected to the strain gauges to read the results. Hydraulic tests are often used to test pressure vessels. To apply internal pressure to the vessel, a hand pump that allowed increasing the pressure up to 1000 bar was used. The pump system was equipped with a hand-held barometer with an accuracy of 10 bar. The stress distribution model obtained from the numerical analysis was used to determine the desired points for installing strain gauges. Due to the geometric symmetry and loading of the vessel, the main directions of stress and strain were along longitudinal and peripheral axes. Thus, strain gauges were installed perpendicular to each other in these directions.

Figures 12 and 13 show the location and installation of the vessel strain gauges. Considering that the welding belt creates a bending moment in the middle of the liner, and this bending moment, according to the sheet and shell theory, causes compressive and tensile stresses up to a certain range of the welding belt, by installing a strain gauge near the welding belt and the connection point of the spherical part to the cylinder, changes in stress and strain is measured.

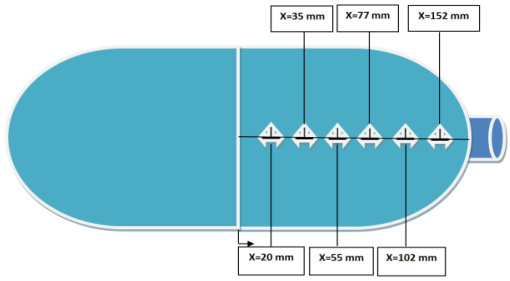

Fig. 12. Location of strain gauges

Fig. 13. Fully filament-wound composite pressure vessels

Figure 14 also presents a schematic representation of the experimental test.

Figures 15 and 16 show the longitudinal and peripheral experimental strain diagrams, respectively. Also, the measurement was started from the middle of the cylindrical part of the vessel to its end.

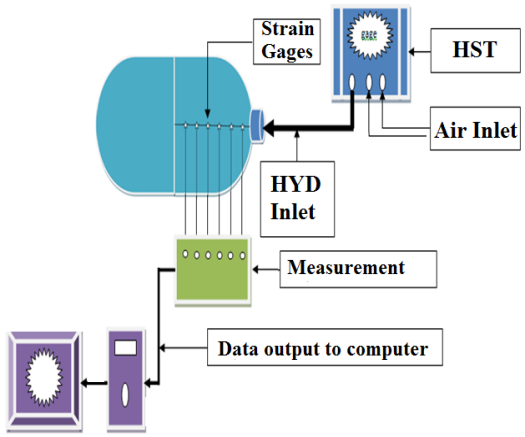

Fig. 14. Schematic of how the vessel was experimentally tested

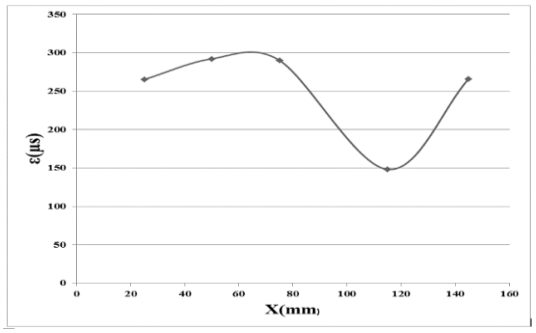

Fig. 15. Experimental strain distribution of the vessel along the longitudinal direction at a pressure of 40 bars

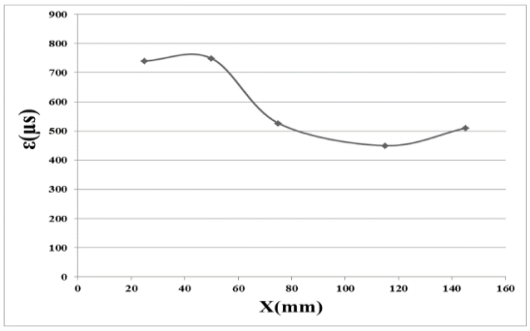

Fig. 16. Experimental strain distribution of the vessel along the peripheral direction at a pressure of 40 bars

The experimental strain was calculated in the previous section, and the relations governing the composites were used to calculate the experimental stress. The angle of the fibers at the locations where the strain gauge is installed and the resulting strain was obtained is used to calculate the stresses. Equations 7 and 8 were used to calculate the stress, and the values obtained for the stresses show good consistency with the numerical results [26].

$$u_z = R_y = R_x = 0 \tag{7}$$

$$u_y = u_x = R_y \tag{8}$$

The longitudinal and peripheral experimental stress diagrams were shown in Figures 17 and

18, respectively. Also, the measurement was started from the middle of the cylindrical part of the vessel to its end.

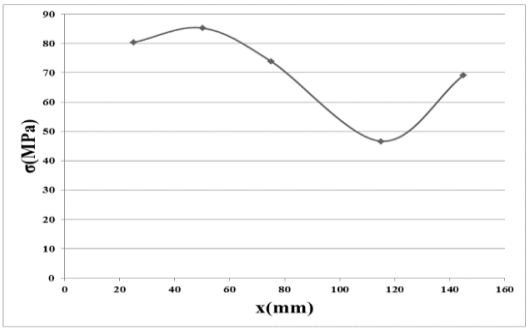

Fig. 17. Experimental stress distribution of the vessel along the longitudinal direction at a pressure of 40 bars

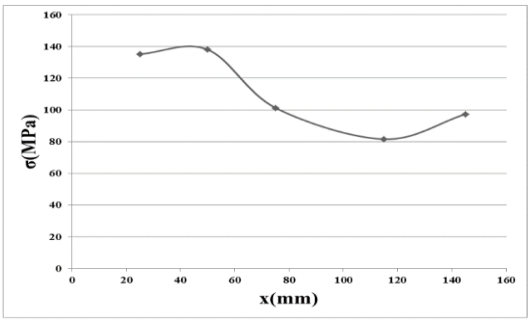

Fig. 18. Experimental stress distribution of the vessel along the peripheral direction at a pressure of 40 bars

4.3. Comparison of Experimental and Numerical Results

Figures 19 and 20 demonstrate the diagrams comparing the longitudinal and peripheral numerical and experimental strain, respectively. The measurement started from the middle of the cylindrical part of the vessel to its end.

Figures 21 and 22 demonstrate the diagrams comparing the longitudinal and peripheral numerical and experimental stress, respectively. The measurement started from the middle of the cylindrical part of the vessel to its end.

As shown in Figures 19 to 22, the stress distribution and strain curves showed similar behavior, as expected. As the diagrams show, the location of the disturbances and the distribution of stress in the longitudinal and peripheral directions follow the strain behavior of the structure.

The performance of the composite vessel under the pressure of 40 bar in numerical and experimental analysis shows that different curves are rather similar. Maximum stress and strain appear at the connection of the cap to the body. By moving away from the edge of the joint in all curves, the curve tends towards uniformity. Based on the diagrams, the overall behavior of the vessel shows consistency with the numerical results. The appearance of the maximum stress on the cylindrical wall and near the joint relates to changes in the geometry and the edge effects in this area.

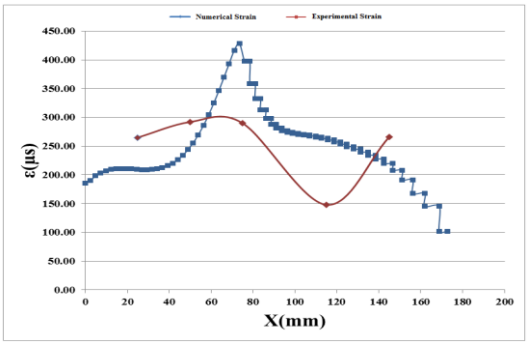

Fig. 19. Comparison of experimental and numerical strain distributions of the vessel along the longitudinal direction at a pressure of 40 bars

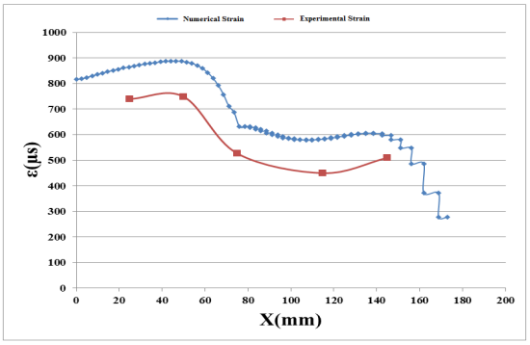

Fig. 20. Comparison of experimental and numerical strain distributions of the vessel along the peripheral direction at a pressure of 40 bars

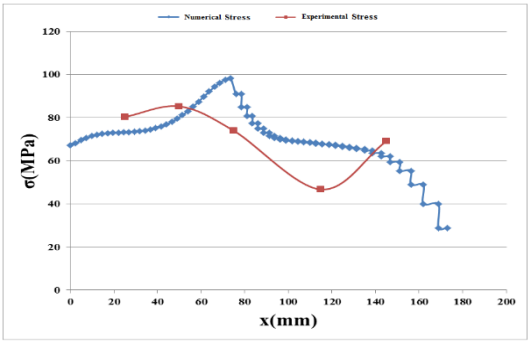

Fig. 21. Comparison of experimental and numerical stress distributions of the vessel along the longitudinal direction at a pressure of 40 bars

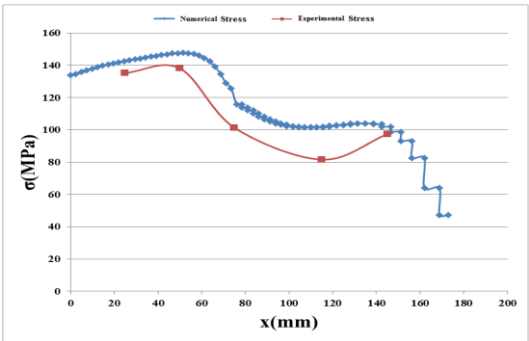

Fig. 22. Comparison of experimental and numerical stress distributions of the vessel along the peripheral direction at a pressure of 40 bars

In the analysis of thin-walled cylinders without a cap under pressure, no axial compressive force is applied to the end of the cap, and only the compression along the radial direction exerted peripheral stress on the cylinder. However, in cylinders with a cap, the compressive force applied to the cap causes an axial tensile force from both sides of the cylinder, which leads to the irregular distribution of stress on the cap and the wall at the joint. By moving away from the joint, the amount of this force decreases and the curve becomes horizontal. Conversely, by moving to the other side of the vessel and approaching the joint, these forces reappear, and the curve gets symmetrical to the center plate of the vessel. The values obtained for stresses and strains at critical points show a difference of 20%, which can be justified by the type of composite used, the quality of materials, and the manufacturing methods that are sometimes far from existing standards.

5. Conclusions

In the present study, a composite vessel possessing a 304 steel liner was designed, and based on this design, the vessel was manufactured. The vessel then was tested under a pressure of 40 bar. The strain was measured using electric strain gauges, and then the stresses were measured. The finite element method was also used to analyze and compare the results. The main findings are as follows:

a) Maximum stress and strain appear at the connection of the cap to the body. By moving away from the edge of the joint in all curves, the curve tends towards uniformity. The appearance of the maximum stress on the cylindrical wall and near the joint relates to changes in the geometry and the edge effects in this area.
b) A change in the geometry of the structure (such as a change in the joint of a spherical part with the cylinder) causes disturbances in the strain and stress curves near the change site.
c) The behavior that the strain curves of a structure show is considered a model of the stress behavior of that structure.
d) It is recommended to model the problem in finite element software to predict the experimental behavior of the structure before performing any experimental test. This saves money and time.
e) The method adopted in this research to model a type III composite vessel meets up to 80% of the designer's expectations. Considering the unavoidable errors such as the creation of bubbles during screw threading, errors in the baking process and errors caused by the angle of fiber placement on the liner, associated with the behavior of the composites, the results of the numerical method can be reliable and acceptable.
f) The method adopted in this research can be used in the construction and testing of vessel liners as well as experimental testing of vessels for industrial applications.
g) This study used an effective and efficient method of experimentally testing the vessel and accumulated sufficient information and experience to carry out a similar study.
h) Considering that 45% of the pressure is borne by the liner, an optimum design of the liner can reduce the liner thickness and reduce the weight of the tank.

References

[1] ISO 11439, 2000. International Standard, Gas cylinders- High Pressure Cylinders for the Onboard Storage of Natural Gas as a Fuel for Automotive Vehicles.
[2] Shen, F.C., 1995. A filament-wound structure technology overview. Materials Chemistry and Physics, 42, pp.96-100.
[3] Heydari, A., 2019. Elasto-Plastic Analysis of Cylindrical Vessel with Arbitrary Material Gradation Subjected to Thermo-Mechanical Loading Via DTM. Arabian Journal for Science and Engineering, 44, pp.8875–8891.
[4] Mallick, P.K., 2007. Fiber-Reinforced Composites: Materials, Manufacturing, and Design, 3rd edtion, Taylor & Francis Group.
[5] Boisse, P., Akkerman, R. & Carlone, P., 2022. Advances in composite forming through 25 years of ESAFORM. International Journal of Material Forming, 15(39).
[6] Dadrasi, A., Shariati, M. & Farzi, G.A., 2022. Experimental, Modeling, and Optimization Investigation on Mechanical Properties and the Crashworthiness of Thin-Walled Frusta of Silica/Epoxy Nano-composites: Fuzzy Neural Network, Particle Swarm Optimization/Multivariate Nonlinear Regression, and Gene Expression Programming. Journal of Materials Engineering and Performance, 31, pp.3030–3040.
[7] Sinha, A.K., Narang H.K. & Bhattacharya, S., 2021. Experimental Determination, Modelling and Prediction of Sliding Wear of Hybrid Polymer Composites Using RSM and Fuzzy Logic. Arabian Journal for Science and Engineering, 46, pp.2071–2082.
[8] Chang, L., Dacheng, Z. & Xinxue, C., 2022. Microstructure Simulation and Experiment for the Weak Weld Joint of a Domed Storage Tank during an Explosion Based on the Cellular Automaton Method. Journal of Materials Engineering and Performance, 31, pp.8094–8112.

[9] Mertiny, P. & Ellyin, F., 2002. Influence of the Filament Winding Tension on Physical and Mechanical Properties of Reinforced Composites. Composite Part A, 33, pp.1615-1622.

[10] Asyraf, M.R.M., Ishak, M.R. & Syamsir, A., 2022. Filament-Wound Glass-Fibre Reinforced PPolymer Composites: Potential Applications for Cross Arm Structure in Transmission Towers. Polymer Bulletin. https://doi.org/10.1007/s00289-022-04114-4

[11] Stabla, P., Lubecki, M. & Smolnicki, M., 2022. The Effect of Mosaic Pattern and Winding Angle on Radially Compressed Filament-Wound CFRP Composite Tubes. Composite Structure, 292(115644).

[12] Azeem, M., HajiYa, H. & Azad Alam, M., 2022. Application of Filament Winding Technology in Composite Pressure Vessels and Challenges: A Review. Journal of Energy Storage, 49(103468).

[13] Thirumavalavan, K. & Sarukasan, D., 2022. Experimental Investigation on Multi-Layered Filament Wound Basalt/E-Glass Hybrid Fiber Composite Tubes. Materials Research Express, 9(4).

[14] Li, H., Liang, Y. & Bao, H., 2007. Splines in the Parameter Domain of Surfaces and Their Application in Filament Winding. Computer Aided Design, 39, pp.268-275.

[15] Kim, C.U., Kang, J.H., Hong, C.S. & Kim, C.G., 2005. Optimal Design of Filament Wound Structures Under Internal Pressure Based on the Semi-geodesic Path Algorithm. Composite Structure, 67, pp.443–452.

[16] Kim, C.U., Kang, J.H., Hong, C.S. & Kim, C.G., 2005. Optimal Design of Filament Wound Type 3 Tanks Under Internal Pressure Using a Modified Genetic Algorithm, Composite Structure, 71, pp.16–25.

[17] Mertiny, P., Ellyin, F. & Hothan, A., 2004. Stacking Sequence Effect of Multi–Angle Filament Wound Tubular Composite Structures. Journal of Composite Materials, 38, pp.1095-1113.

[18] Pei, G., Jingzhong, X. & Qizhia, W., 2021. Analytical Model for Stress and Deformation of Multiple-Winding-Angle Filament-Wound Composite Pipes/vessels Under Multiple Combined Loads. Applied Mathematical Models, 94, pp.576-596.

[19] Polini, W. & Sorrentino, L., 2005. Influence of Winding Speed and Winding Trajectory on Tension in Robotized Filament Winding of Full Section Parts. Composite Science and Technology, 65, pp.1574-1581.

[20] Zhao, L., Mantell, S.C., Cohen, D. & McPeak, R., 2001. Finite Element Modeling of the Filament Winding Process. Composite Structure, 52, pp.499-510.

[21] Choi, J.C., Kim, C. & Jung, S.Y., 2004. Development of an Automated Design System of a CNG Composite Vessel Uusing a Steel Liner Manufactured Using the DDI Process. Journal of Advanced Manufacturing Technology, 24, pp.81–788.

[22] Kabir, M.Z., 2000. Finite Element Analysis of Composite Pressure Vessels with a Load Sharing Metallic Liner. Composite Structure, 49, pp.247-255.

[23] Wang, X., Li, M.D. & Yu, Z.Y., 2001. Self-Strengthening Research of Fiber Reinforced Pressure Vessel with Metallic Liners. Journal of Reinforced Plastics and Composites, 20, pp.1390-1413.

[24] Amraee Rad, G. & Rahimi, G.H., 2021. Design and Analysis of Metal-Composite Vessel Under Internal Pressure. International Journal of Advanced Manufacturing Technology, 14(4), pp.1-10.

[25] Onder, A., Sayman, O., Dogan, T. & Tarakcioglu, N., 2009. Burst Failure Load of Composite Pressure Vessels. Composite Structure, 89, pp.159–166.

[26] Zu, L., Koussios, S. & Beukers, A., 2009. Shape Optimization of Filament Wound Articulated Pressure Vessels Based on Non-Geodesic Trajectories, Composite Structure, 90, pp.339-346.

[27] Koussios, S. & Bergsma, O.K., 2006. Friction Experiments for Filament Winding Application. Journal of Thermoplastic Composite Materials,19, pp.5-34.

[28] Oliveira, L., Hitchcock, D. & Behlow, H., 2014. Second- and Third-Order Elastic Constants of Filaments of HexTow IM7 Carbon Fiber. Journal of Materials Engineering and Performance, 23, pp.685–692.

[29] Dixit, S., Chaudhari, V. & Kulkarni, D.M., 2020. Mode-I Fracture Investigations of Pressure Vessel Steels: Experimental and Simulation Study. Journal of Materials Engineering and Performance, 29, pp.7179–7187.

[30] Labbe, F., 2007. Three-term Asymptotic Stress Field Expansion for Analysis of Surface Cracked Elbows in Nuclear Pressure Vessels. Journal of Materials Engineering and Performance, 16, pp.220–223.